SLICE ALGORITHM - ADVANCED VERSION
METHOD TO FIND SPACE CHARGE FORCES OF HIGH-CURRENT BEAM*

L.G.Vorobiev and R.C.York

National Superconducting Cyclotron Laboratory
Michigan State University
East Lansing, MI 48824

Abstract

A generalization of the slice algorithm introduced in [1,2] for finding the space charge forces of a high-current beam within conducting boundaries is presented. The method now accommodates general beam bunch configurations with different transverse aspect ratios and longitudinal charge density distributions. The central idea of the numerical technique discussed is the discrete representation of a real beam bunch via a sequence of charged disks or slices. By superposition of tabulated template potentials with appropriate interpolation and scaling, the method allows both fast and accurate computation of the space charge potentials for large classes of beam distributions.

I. INTRODUCTION

The three-dimensional (3D) space charge forces of a charged particle beam bunch may be found by analytical methods for only the simplest beam bunch configurations in the absence of conducting boundaries. Numerical recipes such as grid Poisson solvers are required for more general beam distributions within arbitrary conducting chambers. Though these algorithms can in principle be used for any beam shape or conducting chamber geometry, the goal of the procedure discussed in this paper is to develop a much faster but nearly as accurate approach for a large class of beam distributions within relatively simple conducting boundaries.

The main concept of the fast algorithm is the representation of the beam as a sequence of discrete charged disks or slices. The total beam potential is then found by superposition of the individual slice potentials. For the cases explored, this technique has been demonstrated to be both fast and accurate when compared to grid Poisson solvers [1,2]. In the present paper, we generalize the method to accommodate more general beam bunch configurations with different transverse aspect ratios and longitudinal charge density distributions. These generalizations will allow space charge effects for large classes of accelerator configurations to be appropriately simulated.

II. CHARGE DENSITY DISTRIBUTIONS

For two dimensional (2D) transverse charge distributions, we consider rms-matched density profiles based on the concept of equivalent beams (For details see the reference [3] and the bibliography therein).

Consider a two-dimensional charge density distribution that depend on a parameter *p*:

* Work supported by the U.S. Department of Energy Contract # DE-FG02-99ER41118

$$\sigma(x,y,p)=\sigma_m(p)\left(1-\frac{x^2}{x_m^2(p)}-\frac{y^2}{y_m^2(p)}\right)^P \tag{1}$$

where x and y are transverse coordinate variables and $x_m(p)$, $y_m(p)$ and p are distribution variables. This analytic representation allows significant variance of the charge distribution. For most cases ($p>0$) the density is maximal at the beam center with the charge density going to zero near the beam edge. The simplest case ($p=0$) corresponds to a constant charge density. With $p<0$, more exotic beam distributions such as a hollow-beam may also be represented.

The corresponding distribution function $f(x,y,x',y',p)$ also depends on the parameter p. The rms beam size for arbitrary σ as function of (x,y,p) is obtained by integration over (x',y') with normalization.

$$\langle x^2\rangle(p)=\frac{\int\limits_{x,y} x^2\sigma(x,y,p)dxdy}{\int\limits_{x,y}\sigma(x,y,p)dxdy}=\frac{I_1(p)}{I_2(p)} \tag{2}$$

Circular rms-matched transverse charge densities

For the case of a round beam (with notation: $r=\sqrt{x^2+y^2}$ and $r_m=\sqrt{x_m^2+y_m^2}$): $\sigma(r,p)=\sigma_m(p)\left(1-\frac{r^2}{r_m^2(p)}\right)^P$ and the integrals $I_{1,2}(p)$ can be written as:

$$I_1(p)=\sigma_m(p)\int_0^{2\pi}\int_0^{r_m(p)} r^2\cos^2\varphi\left(1-\frac{r^2}{r_m^2(p)}\right)^P rdrd\varphi \text{ and } I_2(p)=\sigma_m(p)\int_0^{2\pi}\int_0^{r_m(p)}\left(1-\frac{r^2}{r_m^2(p)}\right)^P rdrd\varphi$$

resulting in:

$$\langle x^2\rangle(p)=\frac{r_m^2(p)}{2(p+2)} \tag{3}$$

Due to the axial symmetry the same expression is valid for vertical rms-size ($<x^2>=<y^2>$). Noting that $\langle x^2\rangle(0)=r_m^2(0)/4$, for the case of equal transverse rms-sizes for a uniformly charged slice:

$$r_m^2(p)=\frac{(p+2)}{2}r_m^2(0) \tag{4}$$

Given the normalization, $\int\limits_0^{2\pi}\int\limits_0^{r_m(p)}\sigma(r,p)rdrd\varphi=\frac{\sigma_m(p)\pi\, r_m^2(p)}{p+1}\equiv 1$, the maximal value $\sigma_m(p)$ of the 2D charge density is:

$$\sigma_m(p)=\frac{2(p+1)}{p+2}\sigma_m(0) \tag{5}$$

where $\sigma_m(0)$ denotes the charge density for the uniform distribution. For increasing values of p, the shape of a distribution $\sigma(r,p)$ asymptotically gives:

$$\lim_{p\to\infty}\sigma(r,p)=\sigma_m(\infty)\lim_{p\to\infty}\left(1+\frac{-2r^2}{r_m^2(0)(p+2)}\right)^P=\frac{2}{\pi\, r_m^2(0)}\exp\left(-\frac{2r^2}{r_m^2(0)}\right)=\frac{1}{2\pi<x^2>}\exp\left(-\frac{r^2}{2<x^2>}\right)$$

Thus, we obtain in the limit a 2D Gaussian-like charge density distribution, with standard deviation equal to $\sqrt{<x^2>}$ (either horizontal or vertical rms-size of the round beam):

$$\sigma_{EXP}(r)=\frac{1}{2\pi<x^2>}\exp(-\frac{r^2}{2<x^2>})=\sigma(r,\infty)\,.$$

The charge densities $\sigma(r,p)$ from this procedure are plotted in Figure 1 for $p\geq 0$ where the distributions have maximal values at the beam center. For $p = 0$, the distribution is uniform like the KV distribution. The water-bag and parabolic distributions correspond to p=1 and p=2 respectively [3].

Plotted in Figure 2 are charge densities for $p<0$ where $\sigma(r,p=-1)$ (not shown) represents a singular distribution corresponding to the ideal hollow beam. Note that all charge density distributions shown in these figures are rms-matched, i.e. have the same $<x^2>(p)=<y^2>(p)$ for any p, whereas beam maximal sizes depend on p (see equation (4)).

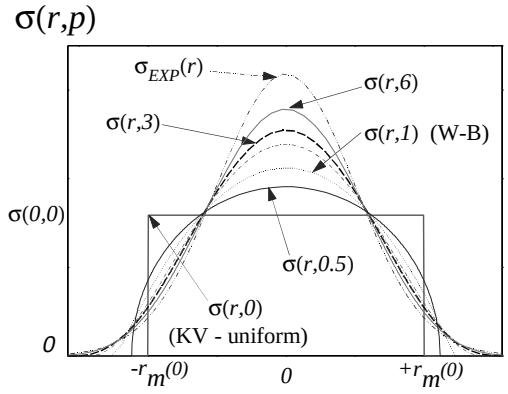

Figure 1. Charge densities $\sigma(r,p)$ as function of radial coordinate r for $p = 0,\ 0.5,\ 1,\ 2,\ 3,\ 6$, and Gaussian shape.

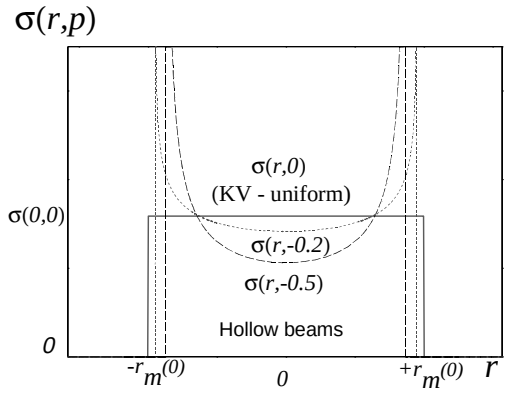

Figure 2. Charge densities $\sigma(r,p)$ as function of r for $p = 0,\ -0.2$ and -0.5.

Elliptical rms-matched transverse charge densities

For the 2D elliptical charge densities: $\left\{(x,y):\ \frac{x^2}{a_x^2}+\frac{y^2}{a_y^2}\le 1\right\}$, with semi-axes ($a_x=\chi\, r_m(s)$ and $a_y=\chi^{-1}r_m(s)$ with the aspect ratio $\chi\neq 1$) by extension of the above formula (2) instead of (3) we obtain:

$$\langle x^2\rangle(p)=\frac{\chi^2\, r_m^2(p)}{2(p+2)} \text{ and } \langle y^2\rangle(p)=\frac{\chi^{-2}\, r_m^2(p)}{2(p+2)}$$

Longitudinal (*z*) line charge densities

A uniform line charge density ($\lambda(z)\equiv const$) of a bunched beam is not particularly physical having a singularity in the field derivative $\partial E_z/\partial z$ at the bunch edges. To analytically describe more physical situations, we introduce a line density function $\Lambda(z)=\lambda_0\cdot\lambda(z)$ where $\lambda(z)$ has a maximum value of 1 and is zero at the bunch ends ($z=\pm z_m$). The parameter λ_0 must satisfy the following normalization criterion:

$$\lambda_0=\frac{J_1}{J_2}=\frac{\int_{-z_m}^{z_m}dz\int_{x,y}\sigma(x,y,z,p)dxdy}{\int_{-z_m}^{z_m}\lambda(z)dz\int_{x,y}\sigma(x,y,z,p)dxdy}$$

where J_1 corresponds to the total charge with the z dependence from $\sigma=\sigma(x,y,z,p)$ via $r_m=r_m(z,p)$.

Note that $\Lambda(z)$ may be *any* function. In practice, we limit ourselves to a family of functions that have a maximum value within the bunch and ramp to zero at the end of the bunch ($z=\pm z_m$). We do not impose other limitations on the behavior of the longitudinal (z) density.

III. SPACE CHARGE POTENTIALS OF 3D BUNCHED BEAMS

Ellipsoid beam bunch with arbitrary transverse and constant line (*z*) charge density

Let us now consider a charged 3D ellipsoid: $\left\{(x,y,z):\ \frac{x^2}{a_x^2}+\frac{y^2}{a_y^2}+\frac{z^2}{a_z^2}\le 1\right\}$ with semi-axes $a_x=a_y=0.01$ m and $a_z=0.1$ m, propagating along a conducting round pipe with radius of $R_{cyl}=0.02$ m and carrying a total charge of $Q_{total}=10^{-11}$ C as shown in Figure 3.

The space charge potential $u(x,y,z)$ within pipe is found from the Poisson equation:

$$\begin{cases} \Delta u(x,y,z) = -4\pi\rho(x,y,z) \\ u(x,y,z)\Big|_{x^2+y^2=R_{cyl}^2} = 0 \quad \text{with} \quad \rho(x,y,z) = \sigma(x,y,z)\Lambda(z) \end{cases}$$

The method to find $u(x,y,z)$ is based on the slice algorithm formalism [1,2]. The transverse density of all slices have transverse charge density profiles as those in Figure 1. So far we assume that the longitudinal (z) density is constant. In Figure 4 the off-axis potentials as functions of (z) at several radial positions (r) and different parameter (p) are given.

At a given radial position, the potentials are similar for $0.5 \le p \le 6$. However, significant variance is seen for the Gaussian distribution as shown on the right hand side of Figure 4. The electric fields $E_z = -\partial u / \partial z$ from the potentials of Figure 4 are given in Figure 5. As anticipated given the similar potential shapes, the electric field dependence on p is relatively weak.

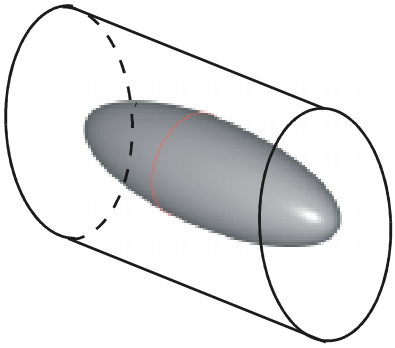

Figure 3. Ellipsoidal beam bunch within a round conducting chamber 4 cm in diameter. The beam in the transverse dimension is round.

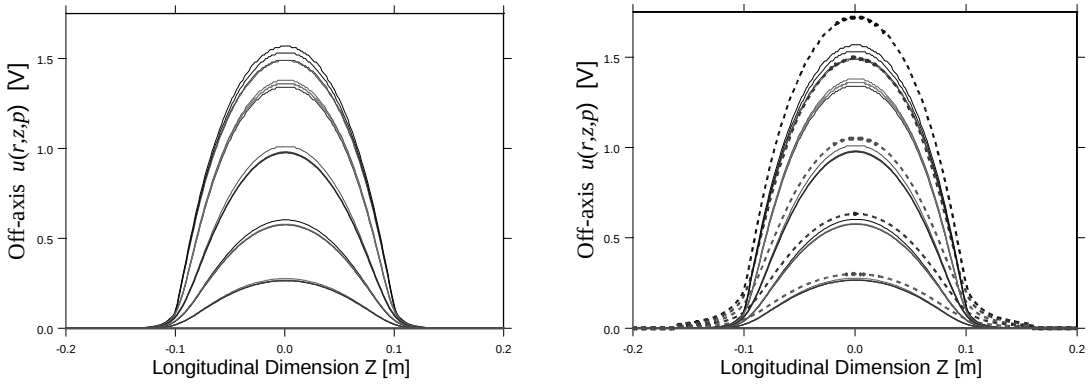

Figure 4. Off-axis potentials $u(r,z,p)$ for different radii r=(0, 0.2, 0.4, 0.6, 0.8, 1)$\times R_{cyl}$ for the beam bunch of Figure 3 for transverse charge densities $\sigma(r,p)$ with $p = 0.5$, 1, 3 and 6 on the left side. On the right hand side the potentials for Gaussian ($p = \infty$) transverse distribution is plotted (dashed lines).

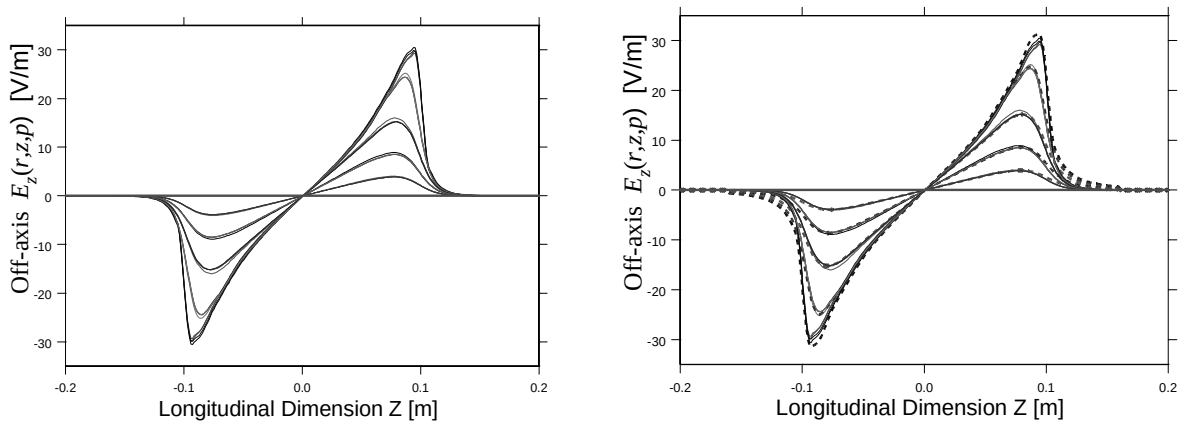

Figure 5. Space charge electrical fields $E_z(r,z,p) = -\dfrac{\partial u(r,z,p)}{\partial z}$ for different radii *r*=(0, 0.2, 0.4, 0.6, 0.8, 1)$\times R_{cyl}$ for the beam bunch of Figure 3 for transverse charge densities $\sigma(r,p)$ with $p = 0.5,\ 1,\ 3$ and 6 on the left side. On the right hand side plotted with dashed lines, the field for the Gaussian distribution is added.

It is important to note that, though the transverse charge distributions vary significantly as shown in Figure 1, there is only relatively modest variance of the potentials given in Figure 4 and even less variation in $E_z(r,z,p)$ as seen in Figure 5. As a consequence, for beams with constant longitudinal (*z*) charge density, the electric field value is relatively insensitive to the radial charge distribution for the parameter p values >0. However for $p \le 0$ the electric field values are significantly more sensitive to the choice of the radial charge distribution as shown in Figure 6.

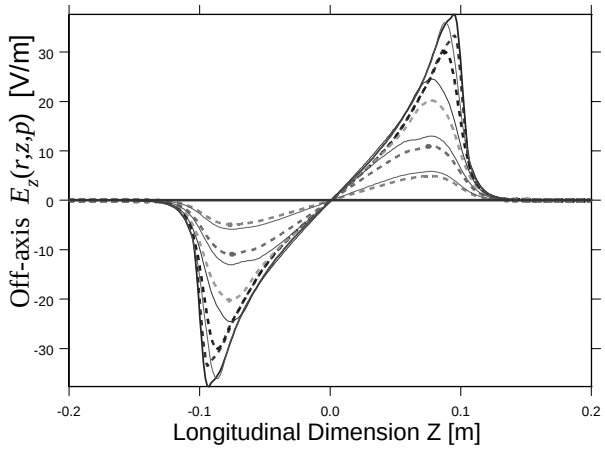

Figure 6. Space charge electrical fields $E_z(r,z,p)$ of the beam bunch of Figure 3 as a function of (*z*) for different radii *r*=(0, 0.2, 0.4, 0.6, 0.8, 1)$\times R_{cyl}$ for $\sigma(r,p)$ with p = -0.2 (solid) and 0 (dashed)**.**

Ellipsoid beam bunch with arbitrary transverse and variable line (*z*) charge density

To evaluate the same charged ellipsoid as in Figure 3 but with varying longitudinal densities, we consider the longitudinal density given by $\Lambda(z) = \lambda_0 \cdot (1 - z^2 / z_m^2)$. The electric fields are given in Figure 7 for transverse charge distributions with p values > 0. The variation is similar to that for constant line (*z*) charge density. Note that the behavior of $E_z(r, z, p)$ at the bunch edges becomes smooth, due to more physical model of $\Lambda(z)$, that also results in no singularity in $\partial E_z / \partial z$.

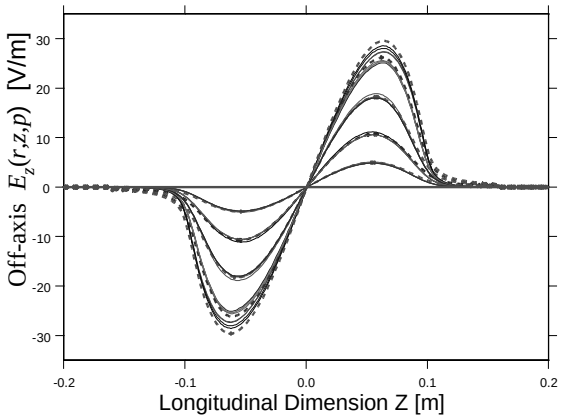

Figure 7. Space charge electrical field $E_z(r, z, p)$ of the beam bunch of Figure 3 with variable longitudinal (*z*) charge density and transverse charge distributions with p values > 0 are at different transverse radii r=(0, 0.2, 0.4, 0.6, 0.8, 1)$\times R_{cyl}$.

The electric fields for transverse charge distributions with p values < 0 are given in Figure 8. Again, the behavior of the fields is more sensitive to the parameter p for transverse charge distributions with p values < 0.

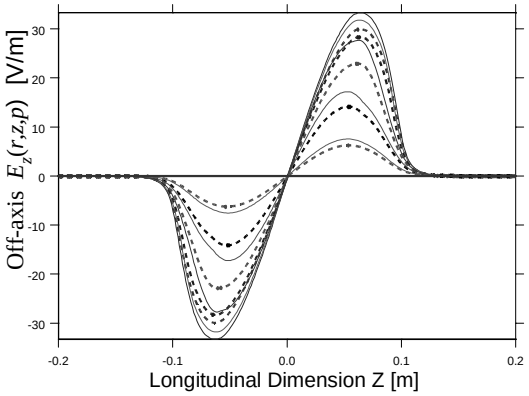

Figure 8. Space charge electrical field $E_z(r, z, p)$ of beam bunch of Figure 3 with variable longitudinal (*z*) charge density and transverse charge distributions with p values < 0 at different transverse radii r=(0, 0.2, 0.4, 0.6, 0.8, 1)$\times R_{cyl}$.

Longitudinally asymmetrical beam bunch with arbitrary density distributions

Beam transported through, for example, a quadrupole focusing channel will have different widths in the horizontal (x) and vertical (y) planes as shown in Figure 9. To properly accommodate this beam condition with the slice algorithm, we generalize round beam formalism.

The general expression for the single slice potential with no axial symmetry is given by general expression [1,2]:

$$u(x_0, y_0, z_0, p) = \iint_{x,y} \frac{\sigma^{slice}(x, y, z, p)dxdydz}{\sqrt{(x-x_0)^2 + (y-y_0)^2 + (z-z_0)^2}}$$

To find image density and image potential on the conducting boundary, we employ the charge density method. However, because of the absence of axial symmetry the dimension of the set of equations in the charge density method becomes proportional to N_φ (see for more details [1,2]) with typical $N_\varphi \cong 100$.

To minimize memory requirements and to increase the speed of calculation, we assume an elliptical shape transversely. Hence, a computational economy may be achieved by performing calculations over only one quadrant, as shown in Figure 9 for azimuthal angles $\alpha \in [0, \pi/2]$. In the absence of a transverse elliptical symmetry, the slice algorithm is inappropriate.

In Figure 10 the space charge potentials and electric fields are shown at azimuthal angles $\alpha = 0, \pi/4, \pi/2$ for the beam bunch of Figure 9 (central plot). For transverse charge density distribution with p = 0.5, 1, 3, 6 and the longitudinal density has the form $\Lambda(z) = \lambda_0 \cdot (1 - z^2/z_m^2)$. The aspect ratio of the transversal cross-section is such ($\chi = \sqrt{2}$) that the beam width is twice the height. The p dependence is minor and both potential and fields: $u(x, y, z, p)$ and $E_z(x, y, z, p)$ are similar to those of a round beam as well as of the both beams with oblate and prolate transversal shapes.

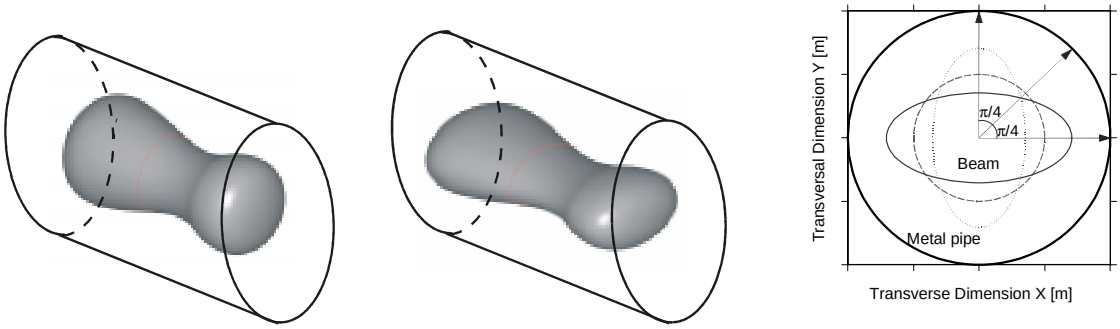

Figure 9. Longitudinally asymmetrical beam bunches within a round conducting chamber 6 cm in diameter (left and central plots). On the right hand side a transversal profile is shown (solid line), the round and prolate beam profiles are plotted as dashed and dotted lines. Due to symmetry, only first quadrant ($\alpha \in [0, \pi/2]$) analysis is required to find potential.

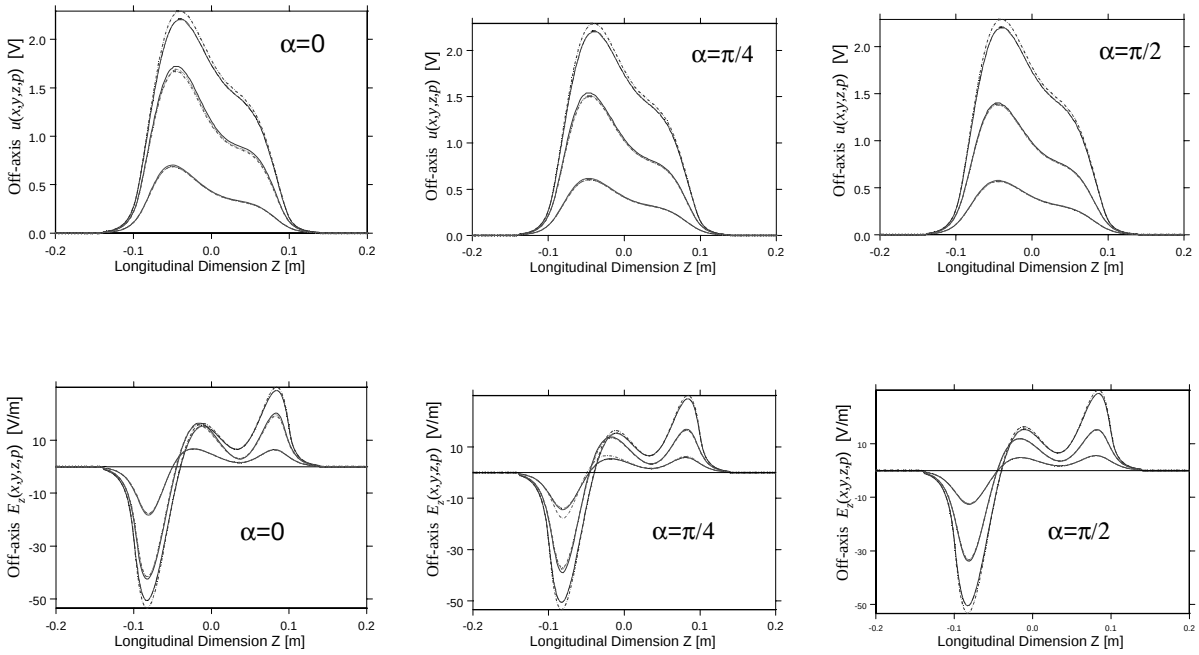

Figure 10. Space charge potentials $u(x, y, z, p)$ and electric fields $E_z(x, y, z, p)$ of the asymmetrical beam bunch from Figure 9 (middle plot) shown along radii $r = (0, 1/3, 2/3, 1) \times R_{cyl}$ with $\alpha = 0,\ \pi/4$ and $\pi/2$. For each plot the transverse charge density was varied with the parameter $p = 0.5,\ 1,\ 3$ and 6 showing a weak sensitivity for both the potential and field behavior. The potential and field of a longitudinally asymmetric beam having axial symmetry (not shown) have very similar behavior.

All numerical results, obtained by the slice algorithm in this section were checked by a general successive over-relaxation three-dimensional (SOR-3D) method. The coincidence between two approaches, for all considered cases, was within a few percents [4].

IV. DISCUSSION AND CONCLUSION

Improvements to the slice algorithm provide fast and accurate computation of the space charge potentials for a large class of bunched beams. The inclusion of image forces due to conducting boundary is the intrinsic feature of the method. The influence of the transverse charge distribution on the longitudinal field was explored. It was found that:

- the values of $E_z(x, y, z, p)$ are relatively insensitive to the value of transverse charge distribution described by the function $\sigma(x, y, z, p)$ for values of $p > 0$.
- for values of $p \le 0$ the sensitivity is greater and care should be taken to avoid errors.

As a beam is propagated through a system the transverse charge density distribution will evolve. Given the relative lack of sensitivity of the E_z electric fields to the details of the transverse charge distribution ($p>0$), it may be possible to only utilize template potentials for only one value of p. Though this assumption will require verification, if valid, would result in only a moderate amount of pre-calculated data given the computational scheme for sub-3D PIC code described in reference 4.

V. REFERENCES

1. L.G.Vorobiev and R.C.York, NSCL/MSU Report-1117, Michigan State University (1998).

2. L.G.Vorobiev and R.C.York, in *Proceedings of the 1999 Particle Accelerator Conference, New York*, edited by A.Luccio and W.MacKay (IEEE, Piscataway, NJ, 1999), p. 2781.

3. M.Reiser "Theory and Design of Charged Particle Beams", John Wiley & Sons, NY, (1994).

4. L.G. Vorobiev and R.C. York, Phys. Rev. ST Accel. Beams **3**, 114201 (2000).